Journal of Instrumentation

Induced radioactivity in ATLAS cavern measured by MPX detector network

Jinst

Published by IOP Publishing for Sissa Medialab

Received: *January 3, 2019*
Accepted: *January 31, 2019*
Published: *March 8, 2019*

Induced radioactivity in ATLAS cavern measured by MPX detector network

M. Campbell,[c] **E. Heijne,**[a,c] **C. Leroy,**[b] **M. Nessi,**[c] **S. Pospisil,**[a] **J. Solc,**[a,d,1] **M. Suk,**[a] **D. Turecek**[a,e] **and Z. Vykydal**[a,d]

[a] *Institute of Experimental and Applied Physics, Czech Technical University in Prague, Horská 3a/22, Praha 2, 128 00 Czech Republic*
[b] *Département de Physique, Université de Montréal, Montréal, Québec, H3C 3J7 Canada*
[c] *CERN, Geneva, Switzerland*
[d] *Czech Metrology Institute, Okruzni 31, Brno, 638 00 Czech Republic*
[e] *ADVACAM s.r.o., U Pergamenky 1145/12, Praha 7, 170 00 Czech Republic*

E-mail: jsolc@cmi.cz

Abstract: An application of the use of MPX detectors for the measurement of induced radioactivity in the Large Hadron Collider (LHC) experiment environment is presented. The sixteen ATLAS-MPX detectors measured the associated photon ambient dose equivalent rate (H*(10) rate) in ATLAS due to the LHC operation. It is presented that in 2010 the average H*(10) rate determined with all MPX detectors varies around 0.015 μSv/h in the ATLAS cavern. In 2013, roughly after 50 days from the end of high luminosity physics runs, the highest H*(10) rate measured with the MPX detectors has reached 14.9 μSv/h (in inner detector region). All the other dedicated MPX detectors measured H*(10) rate which reached the value up to 1.3 μSv/h, depending on the MPX detector.

Keywords: Particle tracking detectors (Solid-state detectors); Dosimetry concepts and apparatus; Pixelated detectors and associated VLSI electronics; Solid state detectors

[1] Corresponding author.

https://doi.org/10.1088/1748-0221/14/03/P03010

2019 JINST 14 P03010

Contents

1 Introduction **1**

2 Materials and methods **1**
2.1 MPX detectors 1
2.2 The method 2
2.2.1 MPX detector calibration in reference photon beams 3
2.2.2 MPX detectors calibration in the environment of natural radiation background 5
2.2.3 LHC induced radioactivity 5

3 Results and discussion **6**

4 Conclusions **8**

2019 JINST 14 P03010

1 Introduction

A network of sixteen MPX pixel detectors (ATLAS-MPX network) based on the Medipix2 chip [1] was installed within the ATLAS experiment at CERN, see page 50 in [2]. Their location is illustrated in figure 1 with their coordinates given in table 1. A detailed description of the ATLAS-MPX detectors network and operation can be found in [3] and [4].

The present paper reports an example of application of MPX detectors. It consists of the measurement of the photon ambient dose equivalent rate (H*(10) rate) performed with the MPX detectors during the period before the start of LHC collisions in 2010 and after the LHC shutdown in 2013. The number of interacting photons and electrons in the detectors was determined from the amount of measured clusters/tracks produced by corresponding radiation quanta in the pixelated sensor. The cluster rate was recalculated into H*(10) rate utilizing a conversion coefficient determined from an MPX detector of reference exposed to gamma ray sources (^{60}Co and ^{137}Cs) of known H*(10) rate. The value of the conversion coefficient was confirmed by two independent methods: by MCNPX™ Monte Carlo simulation modelling the experimental set-up of reference and by comparing the MPX detector response to natural radiation background in Prague with the reading of a calibrated dosimeter.

2 Materials and methods

2.1 MPX detectors

The utilized MPX device consists of a 300 μm thick silicon sensor matrix of 256 × 256 cells (matrix element 55 × 55 μm^2) bump-bonded to a pixelated read-out chip. Each MPX device is fitted in a duralumin box with an entrance window located above the sensor. The network detectors were operated in tracking mode with low threshold (8–10 keV). The signature of particles interacting

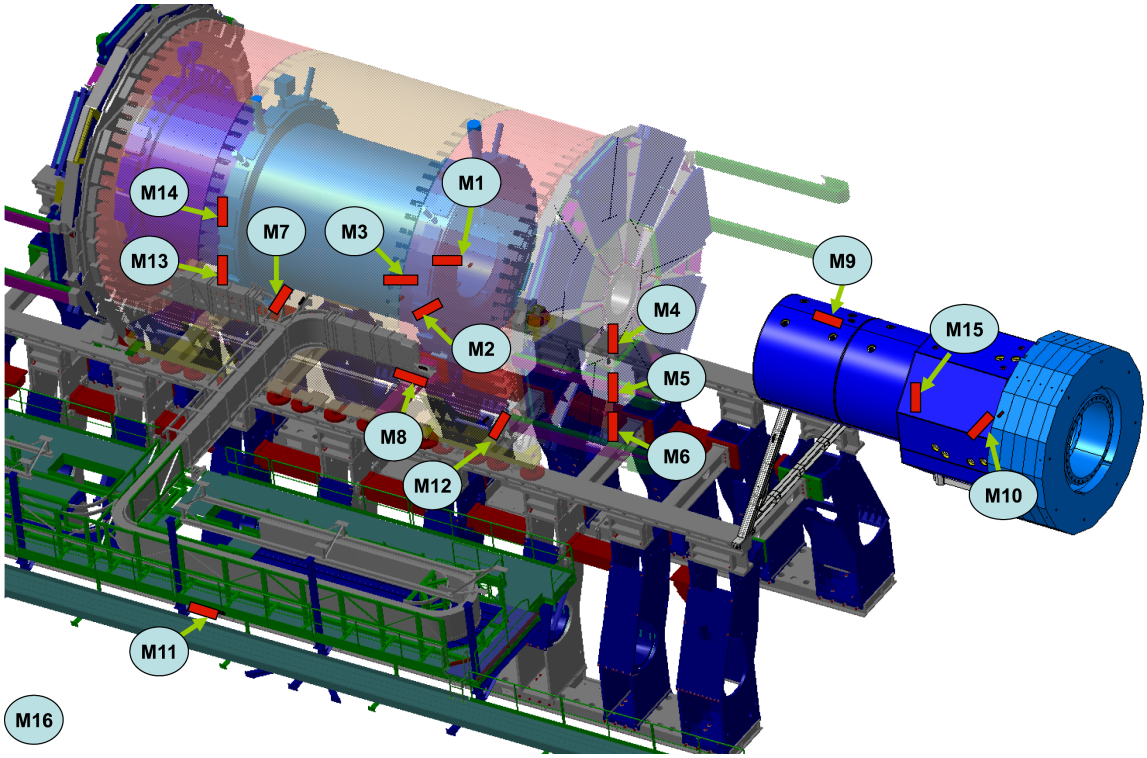

Figure 1. Location of the MPX detectors in ATLAS.

in the silicon layer is visualized in the form of a cluster of adjoining activated pixels (a track), similarly to nuclear emulsion with different size and shape depending on the type of particles, their energies, incidence angles, and the nature of their interactions in the sensor. The remotely settable integration time window (depending on the luminosity and the MPX position in ATLAS) was set short enough to avoid overlap of tracks created by the individual particles. The integration times were in the range from 10 ms to 30 s. Data collected in the tracking mode were analyzed with a pattern recognition algorithm [3] and subsequently stored for further evaluation.

2.2 The method

The MPX detector does not measure directly the energy deposited by the particles. However, based on the cluster shape analysis it can provide the composition of the radiation field, i.e., the particle types and their approximate energy ranges [3]. Then, it can measure the radiation field composed of natural radiation background and LHC induced radioactivity (due to decay of radioactive nuclei generated in the ATLAS environment during LHC collisions), see pages 51–52 in [2]. After an LHC collision period, this radiation field primarily consists of photons and electrons with prevailing energy between few hundreds of keV and few MeV. Figure 2 shows examples of measurement of such radiation fields with MPX detectors between 6 and 9 December 2012. The interpretation of the measurement of these induced radiation fields is simpler than that of the complex radiation field generated during LHC collisions [3, 4]. Using a calibration with standardized photon beams in that energy range, it was possible to calculate the H*(10) rate from the measured cluster rate.

2019 JINST 14 P03010

Table 1. MPX detector locations and positions with respect to the central interaction point. X, Y and Z axes correspond to the standard ATLAS coordinate system, R = $(X^2 + Y^2)^{1/2}$ is the distance from the beam axis at position Z. The approximate orientation of the devices is given with respect to the beam axis (Z-axis) with the sensitive surface of the detectors facing the interaction point. Z determines beam direction, positive sign corresponds to side A, negative to side C, Y — positive sign corresponds to up direction, negative to down, X — positive corresponds to orientation toward the center of the LHC ring, negative toward U.S.A. 15 (outside the ring). (0, 0, 0) are the coordinates of the interaction point.

(ID = Inner Detector, JM plug = Moderator Shielding, TILE/TILECAL = Tile Calorimeter, EB = Extended Barrel Tile Calorimeter, Small Wheel = part of the Muon Spectrometer, JF = Forward Shielding, HO = visitors gallery in ATLAS Cavern, level 4, U.S.A. side, EIL 4 = End-cap inner large (muon chamber), LUCID = Luminosity detector, U.S.A. 15 = Underground Service Area) [2].

Detector	Location description	X [m]	Y [m]	Z [m]	R [m]	Orientation
MPX01	between ID and JM plug	−0.71	0.29	3.42	0.77	90°
MPX02	between TILE and EB	−2.23	−1.12	3.42	2.50	90°
MPX03	between TILE and EB	−3.45	0.93	2.94	3.57	90°
MPX04	on the Small Wheel	−0.65	−1.30	7.12	1.30	90°
MPX05	on the Small Wheel	−0.55	−2.36	7.20	2.36	90°
MPX06	on the Small Wheel	−0.65	−3.36	7.20	3.36	90°
MPX07	top of TILECAL barrel	−4.53	0.79	0.35	4.59	90°
MPX08	top of TILECAL EB	−4.37	−0.53	4.02	4.40	0°
MPX09	on the JF cylinder	0.00	1.56	15.39	1.56	0°
MPX10	cavern wall HO	−3.96	3.36	22.88	5.19	45°
MPX11	cavern wall U.S.A. side	−16.69	0.05	4.86	16.69	0°
MPX12	on the EIL 4	−6.25	0.00	7.23	6.25	90°
MPX13	between TILE and EB, C	−2.21	−1.02	−3.42	2.44	90°
MPX14	between ID and JM plug, C	−0.71	−0.30	−3.43	0.77	90°
MPX15	at the back of LUCID	0.19	−0.08	18.74	0.20	90°
MPX16	U.S.A. 15	−39.48	0.90	−6.55	39.48	N/A

2.2.1 MPX detector calibration in reference photon beams

It has been experimentally confirmed that the MPX detector response to photons and charged particles is consistent from detector to detector within 20% [3]. Therefore, only one reference device was exploited for the H*(10) rate calibration. For the calibration, the standardized ^{137}Cs and ^{60}Co photon beams (divergent collimated fields of point-like sources) available in the Czech Metrology Institute in Prague were used. The energies of photons emitted in the process of the radionuclides disintegration are observed to correspond roughly to the mean energies of natural radiation background and expected LHC induced radioactivity in the ATLAS environment.

During the calibration procedure, the detector was positioned perpendicularly to the ^{60}Co and ^{137}Cs photon beam axis, 300 cm from the source, and irradiated from the front side and then from the back side. To keep calibration conditions close to the ATLAS radiation conditions, the detector was calibrated without its duralumin box so the electrons created in the air and surroundings could contribute to the measured signal as well, in addition to electrons created directly inside the sensor

2019 JINST 14 P03010

chip. To obtain the calibration coefficient for ^{60}Co and ^{137}Cs, the reference H*(10) rate of the corresponding photon beam at the MPX detector calibration position was divided by the rate of all clusters registered on the whole area of the sensor.

Monte Carlo simulations were performed in order to cross-check the measurement results. The geometry of the experiment, including the shape and composition of MPX devices [3, 4], was modeled in the MCNPX™ code [5]. The simulations were performed for both photon beams and for a detector without a duralumin box (as in the calibration experiment), with a duralumin box (as in ATLAS), and with a duralumin box without an entrance window in the box (with the aim to estimate differences on detector sensitivity with entrance window oriented either to open space or to wall of box fixation). Table 2 presents the comparison between measured and simulated values of the conversion coefficient.

Table 2. Summary of the measured and simulated calibration coefficient converting the cluster rates into H*(10) rate. The statistical uncertainty on the simulation and measurement is 1.5% and 3.0%, respectively.

Detector, geometry	**Conversion coefficient [$\times 10^{-10}$ Sv/cluster]**	
	^{60}Co photon beam	**^{137}Cs photon beam**
irradiation from the front side		
Measurement, no box	2.29	1.72
Simulation, no box	2.55	1.90
Simulation, box	2.39	1.74
Simulation, box, no entrance window	2.24	1.73
irradiation from the back side		
Measurement, no box	2.39	1.79
Simulation, no box	2.68	1.97
Simulation, box	2.75	2.05
Simulation, box, no entrance window	2.68	2.02

It can be concluded from table 2 that the value of the calibration coefficient is slightly dependent on both the orientation of the detector and photon energy. However, the differences between measured and simulated coefficients as well as their variation are within 15%. Therefore, we chose to set the calibration coefficient converting the cluster rate into H*(10) rate to the value of $\mathbf{2.0 \times 10^{-10}}$ **Sv/cluster**. Assuming that the induced radiation field in ATLAS is close to be isotropic and taking into account the MPX detector energy-angular detection efficiency for photons [3], one can expect that the angular dependence of the conversion coefficient is also well within 15%. The value is valid for the MPX detectors in tracking mode of operation at low threshold, and for the cluster rate obtained from the whole area of the sensor.

The difference observed between simulated and measured conversion coefficients could be caused by an over-simplification of the model, which neglected scattering objects, like irradiation hall walls and floor or a detector holder. Also, the discrepancy could be caused by the difference between the real photon fluence spectra and the ones utilized in the simulations. Taking into

2019 JINST 14 P03010

account the over-simplifications, the agreement between simulation and measurement is satisfactory. Therefore, one can conclude that the simulation confirmed the value of the conversion coefficient determined by the experiment.

It can be also concluded that the conversion coefficient does not significantly depend on the cover of the detector. The difference between the conversion coefficient for a detector without a box, inside a box, or inside a box but without an entrance window is lower than 10%.

2.2.2 MPX detectors calibration in the environment of natural radiation background

To certify the calibration, the simultaneous measurement of the H*(10) rate of natural radiation background was performed inside the Institute of Experimental and Applied Physics (IEAP) in Prague during August 2013 with MPX03, MPX08, MPX10, MPX12, and MPX16 (taken out of the ATLAS cavern for this purpose) and with two certified electronic dosimeters UltraRadiac™ (Canberra). Table 3 summarizes the comparison between the H*(10) rates of natural radiation background as measured by the MPX detectors and the UltraRadiac™ dosimeters.

Table 3. Average H*(10) rate of natural radiation background at IEAP building, Prague, as measured by MPX detectors and dosimeters UltraRadiac™. Experiment 1 was performed on 8 August 2013, experiment 2 took place from 9 to 10 August 2013. The calibration coefficient value of 2.0×10^{-10} Sv/cluster was used for MPX detectors data.

Experiment	Detector	H*(10) rate [μSv/h]
1	MPX03	0.165
	MPX10	0.155
	UltraRadiac™, device 1	0.158
2	MPX08	0.162
	MPX12	0.164
	MPX16	0.162
	UltraRadiac™, device 1	0.160
	UltraRadiac™, device 2	0.166

A very good agreement was found between all MPX detectors and both UltraRadiac™ dosimeters. The H*(10) rates agree within 3%, which is at the level of statistical uncertainty on the measurements and fluctuations of the natural radiation background. The comparative experiment proved that the calibration coefficient of 2.0×10^{-10} Sv/cluster is valid also for the natural radiation background at ground level.

2.2.3 LHC induced radioactivity

The similarity between the photon calibration field and the natural radiation background with LHC induced radioactivity field has to be demonstrated for justifying the use of the value of the conversion coefficient stated above. Figure 3 presents an example of MPX frames acquired under exposure of a) the MPX detector of reference to ^{60}Co photon beam, b) the MPX03 to ^{137}Cs source during the Tile Calorimeter inter-calibration in ATLAS on 3 August 2010 [3, 6], c) the MPX03 to natural radiation background at Prague on 8 August 2013, and d) the MPX03 to LHC induced radioactivity on 17 February 2013. The frame length (acquisition time) was adjusted according to a count rate to

2019 JINST 14 P03010

minimize the number of overlapping tracks in frame. For the calibration with ^{60}Co, as an example, the frame length was set to 0.1 ms at dose rate 0.1 Sv/h and 1 s at 10 µSv/h. The structure and the distribution of lengths of clusters in all frames are quite similar.

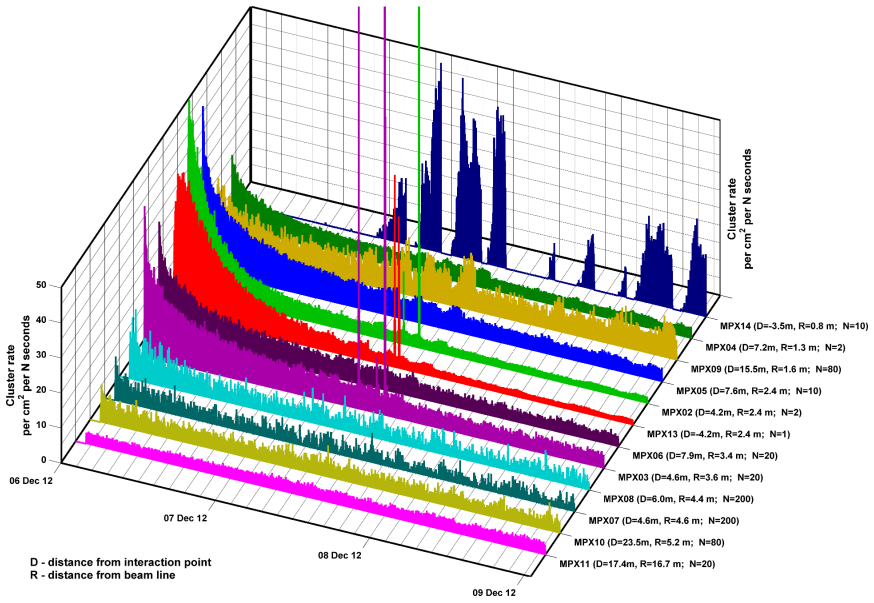

Figure 2. Example of LHC induced radioactivity as measured with MPX detectors between 6 and 9 December 2012. Cluster rates in each MPX detector are multiplied by the value N for data scaling. MPX14 data do not represent induced radioactivity but referred to as HETP — High Energy Transfer Particles in our previous papers ([3, 4]) generated during either beam collisions or some beam operations, as this detector was set at high threshold [3], being insensitive to LETP (Low Energy Transfer Particles [3, 4] — specifically to electrons and photons). The beam operations recorded with MPX14 justify the bumps visible in several other MPX detectors. Sharp peaks occurred at several MPX detectors between 7 and 8 December correspond to Tile Calorimeter inter-calibrations with a ^{137}Cs source. See also figure 4.

Table 4 summarizes the fractions of different types of clusters in calibration data and radiation background measurements. A measurement with an ^{241}Am source emitting 59.5 keV photons is included in the table to show the ratio of clusters that resulted in low energy photon field. Comparing the data in table 4, it can be said that the LHC induced radioactivity field in ATLAS after 50 days of "cooling", after the end of high luminosity physics runs, is similar to the natural radiation background. It is also similar to ^{137}Cs photon field but it includes slightly more dots (clusters of one pixel), i.e., more low energy photons (tens of keV) are detected. One can conclude that the spectral composition of LHC induced radioactivity in ATLAS is rather close to that of natural radiation background which justifies the use of the value of the calibration coefficient stated above for determination of H*(10) rate caused by LHC induced radioactivity.

3 Results and discussion

Table 5 presents the H*(10) rates caused by the natural radiation background and LHC induced radioactivity in the ATLAS cavern, as measured by the MPX detectors in February 2013, roughly after 50 days of "cooling". For comparison, data from the beginning of February 2010, before the

2019 JINST 14 P03010

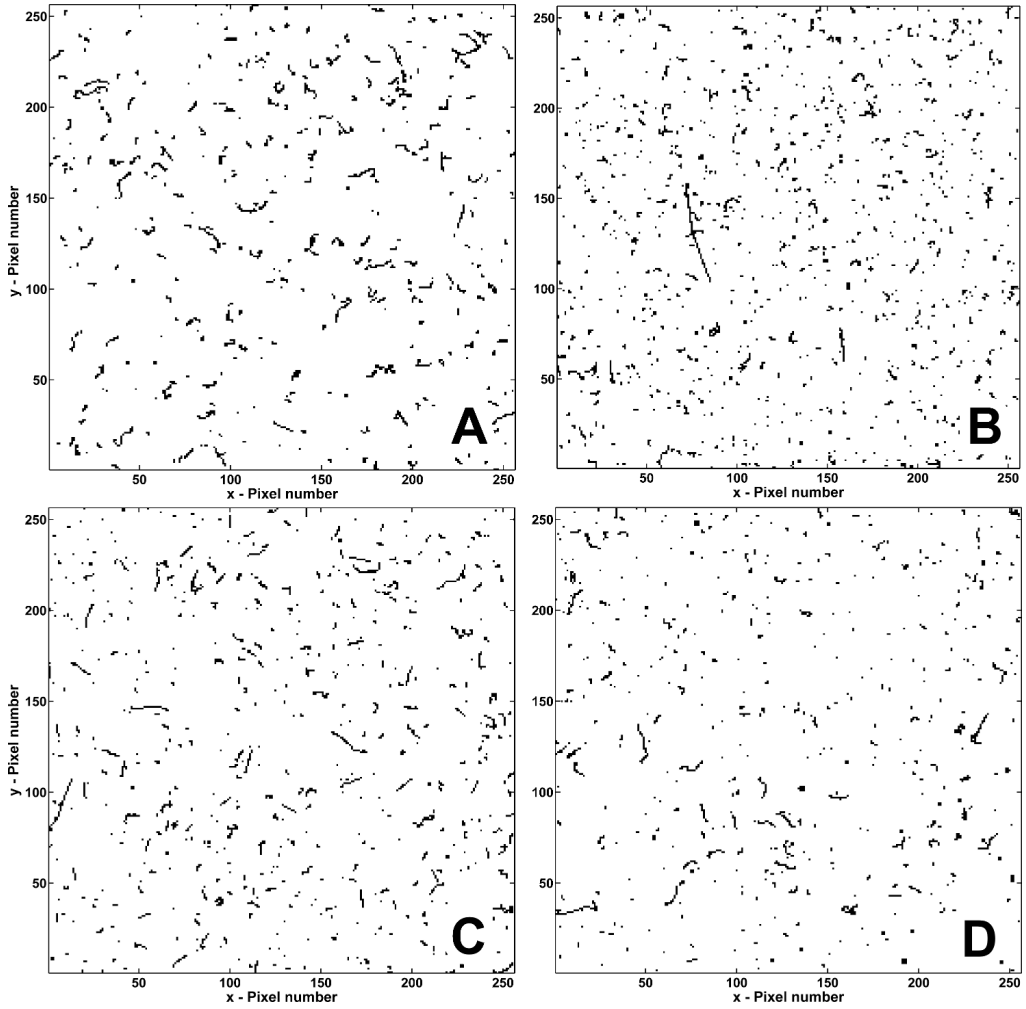

Figure 3. An example of frames acquired in various radiation fields dominated by photons and electrons: A — MPX detector of reference frame acquired with a ^{60}Co photon beam exposure (mean energy 1.25 MeV); B — MPX03 frame acquired during the Tile Calorimeter inter-calibration performed with a ^{137}Cs source (662 keV) on 7 December 2012 (see also figure 4); C — integrated frame of MPX03 during measurement of natural radiation background at IEAP in Prague on 8 August 2013; D — integrated frame of MPX03 during no LHC collisions, 17 February 2013. All clusters are created by electrons originated in photo-atomic interactions in the MPX sensor itself and in surrounding environment. The exposure times were chosen to be 0.1 ms and 1 s for 0.1 Gy/h and 10^{-5} Gy/h, respectively, so that during the calibration there were not more than 14 tracks per frame to avoid tracks overlap.

LHC collisions started, are given as well. The ATLAS recorded total integrated luminosity in 2012 was 21.79 fb^{-1} [7].

The H*(10) rates measured by MPX detectors in 2010 are consistent between each other and they correspond to expected level of natural radiation background in ATLAS cavern located 92 m below the ground (cavern floor level; the cavern height is 35 m [8]). The H*(10) rates are about one order of magnitude lower than those at the ground. The higher H*(10) rate in MPX10 and MPX11 compared to other MPX detectors is most likely caused by natural radioactivity in the concrete because these detectors were mounted onto a concrete wall. Other slight variations in the detector

2019 JINST 14 P03010

Table 4. Distribution of diverse types of clusters measured in different radiation fields dominated by photons and electrons, as obtained from cluster pattern recognition analysis [3]. Dots: cluster of one pixel; Small blob: cluster of 2–4 pixels; Curly track: cluster with a shape of a curly line of more than 4 pixels in length.

Cluster type	^{241}Am calibration field[1]	^{137}Cs calibration field[2]	^{60}Co calibration field[3]	Natural background[4]	MPX03, 7–13 Jan 2010[5]	MPX03, 17 Feb 2013[6]	MPX13, 7–13 Jan 2010[5]	MPX13, 15 Feb 2013[6]
Dots	61%	25%	17%	38%	47%	43%	48%	43%
Small blobs	38%	36%	28%	30%	21%	31%	26%	30%
Curly tracks	1%	39%	55%	32%	32%	26%	26%	27%

[1]Energy 59.5 keV.
[2]Energy 662 keV.
[3]Mean energy 1.25 MeV.
[4]Inside IEAP building in Prague on 8 August 2013.
[5]Before LHC collisions started.
[6]After LHC shutdown.

responses result from variations of the radiation field according to the environment surrounding each MPX detector.

It is seen from table 5 that in February 2013 the contribution of the LHC induced radioactivity with long half-life became negligible at the positions of MPX07 to MPX11. On the other hand, the highest H*(10) caused by this long half-life component of induced radioactivity was measured by MPX01 (14.9 μSv/h) and was indirectly estimated in MPX14 (14 μSv/h) and MPX15 (225 μSv/h).

There have been several Monte Carlo studies [9, 10] and another direct measurement of the induced radioactivity in ATLAS [11]. Table 5 reports the H*(10) rates as measured by several MPX detectors in February 2013, approximately after 50 days of "cooling". However, a sensible comparison with the results of [12] was not possible as both types of detectors were located in different positions and the amount and composition of material in between and around them was different. The locations of MPX detectors in ATLAS system are reported in table 1.

As an example, the decay of the LHC induced radioactivity with short half-life within a few days is presented in figure 4. The MPX03 cluster rate per frame and the corresponding H*(10) rate is shown for a time period of 5 days starting just after the end of LHC collisions on 6 December 2012.

4 Conclusions

The induced radioactivity and associated photon ambient dose equivalent rate (H*(10) rate) in ATLAS due to the Large Hadron Collider (LHC) operation was obtained from measurements with ATLAS-MPX silicon pixel detectors (MPX detectors). It was demonstrated that the ATLAS-MPX network, consisting of 16 MPX detectors, delivers on-line information about radiation level across the whole ATLAS detector during and after LHC collision periods. In 2013, roughly after 50 days of "cooling", the highest H*(10) rate measured with MPX detectors dedicated to radioactivity measurement inside the ATLAS detector was obtained with MPX01 located between the JM plug shielding and the inner detector reaching 14.9 μSv/h. For all the other dedicated MPX detectors, the H*(10) rate reached a value up to 1.3 μSv/h, depending on the detector position.

The currently installed ATLAS-TPX network [13] (upgraded version of ATLAS-MPX network) has also the capability, as the MPX detector network, to determine induced radioactivity in a broad

2019 JINST 14 P03010

Table 5. Summary of average H*(10) rates measured by all MPX detectors in February 2010 and February 2013. Statistical uncertainty of the measurements (number of registered clusters) is below 3%.

Detector	Measurements in 2013		Measurements in 2010	
	Date	H*(10) rate [μSv/h]	Date	H*(10) rate [μSv/h]
MPX01	3 Feb	14.9	28 Jan–4 Feb	0.012
MPX02	15 Feb	0.368	29 Jan–13 Feb[1]	0.008
MPX03	17 Feb	0.080	28 Jan–4 Feb	0.008
MPX04	17 Feb	0.500	28 Jan–4 Feb	0.011
MPX05	17 Feb	0.104	28 Jan–4 Feb	0.012
MPX06	17 Feb	0.050	28 Jan–4 Feb	0.015
MPX07	2 Feb	0.010	28 Jan–4 Feb	0.011
MPX08	2 Feb	0.011	28 Jan–4 Feb	0.008
MPX09	2 Feb	0.036	28 Jan–4 Feb	0.018
MPX10	2 Feb	0.046	28 Jan–4 Feb	0.041
MPX11	31 Jan	0.050	28 Jan–4 Feb	0.040
MPX12	31 Jan	0.051	29 Jan–4 Feb	0.014
MPX13	15 Feb	1.32	28 Jan–4 Feb	0.009
MPX14	—	14,[2]	28 Jan–4 Feb	0.012
MPX15	—	225,[2]	28 Jan–4 Feb	0.014
MPX16	25 Jan	0.022	24 Feb–29 Mar	0.015

[1]Data from 2011 because MPX02 was not in operation in 2010.

[2]These detectors were set in high threshold [3] from March 2011, being insensitive to photons and electrons. Values are estimates based on the ratio of H*(10) of MPX14 and MPX15 over MPX01 in February 2011, after 90 days of "cooling" (after the end of 2010 collisions).

range of decay half-lives, from minutes to years (table 5, reference [3]). The capability of MPX and now TPX network can be utilized for instance to predict growth and decay of the LHC induced radioactivity based on the measured data a) to estimate its contribution to ATLAS radiation field during LHC collisions and b) to predict the H*(10) rate any time ahead according the expected LHC schedule.

Acknowledgments

We thank Ludmila Stemberkova and Vladimir Sochor from the Czech Metrology Institute, Regional Branch Prague, Czech Republic, for their help with the MPX detector calibration in photon beams and with the UltraRadiac™ detector response verification in the low background chamber. We also thank the ATLAS Technical Coordinator and ATLAS Spokesperson for supporting this project.

The project was supported by the Ministry of Education, Youth and Sports of the Czech Republic under projects number MSM 68400029, LA 08032 and LG 13009. The work was supported from European Regional Development Fund-Project "Engineering applications of microworld physics" (No. CZ.02.1.01/0.0/0.0/16_019/0000766) and from the European Regional Development Fund-Project "Van de Graaff Accelerator — a Tunable Source of Monoenergetic Neutrons and Light

2019 JINST 14 P03010

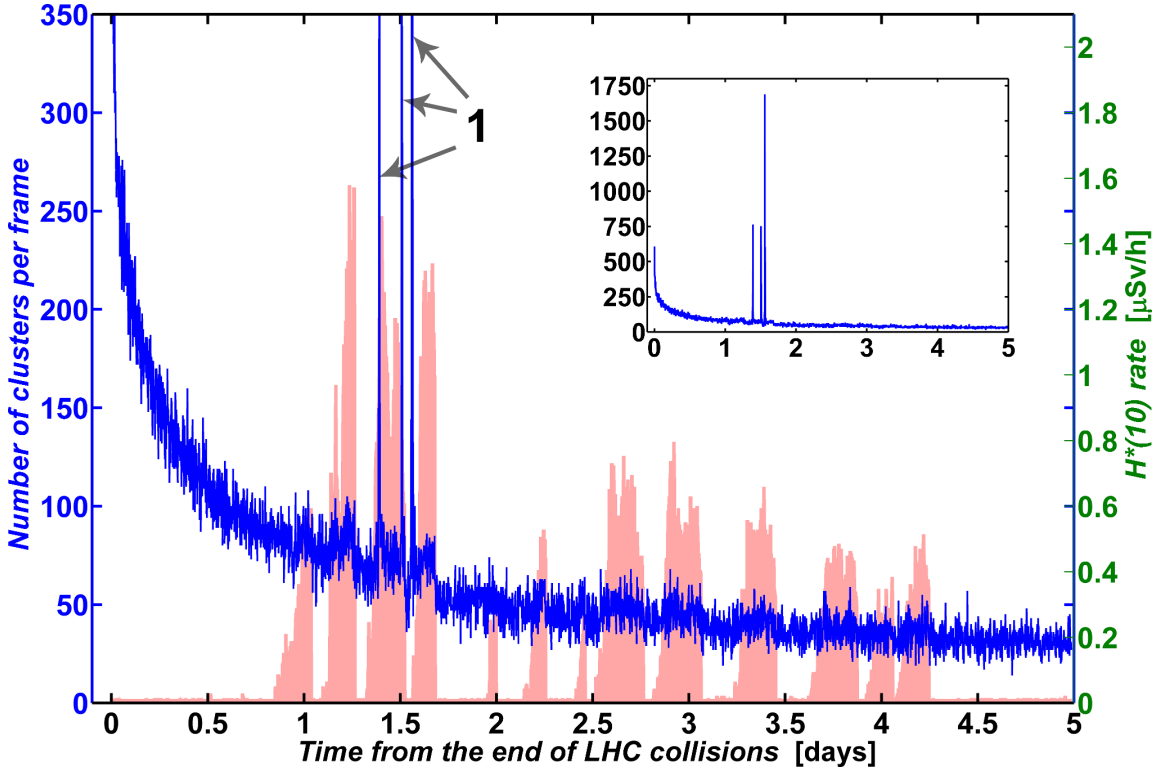

Figure 4. An example of LHC induced radioactivity measured by MPX03 during 5 days starting from 6 December 2012 (blue line). The H*(10) rate is indicated on the right hand side. The peaks marked by the number 1 are caused by a ^{137}Cs source used for the Tile Calorimeter inter-calibration performed on 7 December between 9:50 and 14:25 GMT. The full range of the cluster rate per frame measured during the ^{137}Cs scans is shown in the inset. Several bumps are visible on the blue curve, which are probably caused by some beam activities. This assumption is based on the observation of signal of MPX14 device displayed as pink areas (relative scale). This device, positioned close to the interaction point, is set at high threshold [3], being sensitive to fast neutrons and highly ionizing particles (i.e., High Energy Transfer Particles-HETP) generated during beam collisions only.

Ions" (No. CZ.02.1.01/0.0/0.0/16_013/0001785). The project was also supported by the Natural Sciences and Engineering Research Council of Canada (NSERC).

References

[1] Medipix collaboration, (2019) http://www.cern.ch/medipix.

[2] ATLAS collaboration, *The ATLAS Experiment at the CERN Large Hadron Collider*, in *The CERN Large Hadron Collider: Accelerator and Experiments. Volume 1: LHC Machine, Alice and ATLAS*, A. Breskin and R. Voss eds., CERN, Geneva Switzerland (2009) [ISBN: 978–92/9083–337–6] [2008 *JINST* **3** S08003].

[3] ATLAS collaboration, *Analysis of the Radiation Field in ATLAS Using 2008 2011 Data from the ATLAS-MPX Network*, ATL-GEN-PUB-2013-001 (2013).

[4] E. Heijne et al., *Comparison of Measurement and Simulation of ATLAS Cavern Radiation Background*, ATL-COM-GEN-2013-003.

2019 JINST 14 P03010

[5] D.B. Pelowitz et al., *MCNPX™ 2.7.E extensions*, LA-UR-11-01502 (2011).

[6] ATLAS collaboration, *Cesium monitoring system for ATLAS Tile Hadron Calorimeter*, *Nucl. Instrum. Meth.* **A 494** (2002) 381.

[7] *ATLAS Experiment: Luminosity Public Results*, (2018) https://twiki.cern.ch/twiki/bin/view/AtlasPublic/LuminosityPublicResults.

[8] *ATLAS Experiment: Fact Shee*, (2019) http://atlasexperiment.org/fact-sheets.html.

[9] V. Hedberg, *Induced radioactivity in the ATLAS experiment — An update*, RPC/2003/XXXVIII/137 (2003).

[10] V. Hedberg, M. Magistris, M.N. Morev, M. Silari and Z. Zajacová, *Predicting induced radioactivity in a large high-energy physics apparatus: The example of the ATLAS experiment*, *Nucl. Instrum. Meth.* **A 592** (2008) 230.

[11] O. Beltramello, *ATLAS Radiation Protection issues and strategy LS3 and Later*, talk given at *Forum on Tracking Detector Mechanics 2013*, Oxford, U.K., 19–21 June 2013.

[12] C. Leroy, S. Pospisil, M. Suk, and Z. Vykydal, *Proposal to Measure Radiation Field Characteristics, Luminosity and Induced Radioactivity in ATLAS with TIMEPIX Devices*, ATLAS-COM-GEN-2014-005 (2014).

[13] B. Bergmann, I. Caicedo, C. Leroy, S. Pospisil and Z. Vykydal, *ATLAS-TPX: a two-layer pixel detector setup for neutron detection and radiation field characterization*, 2016 *JINST* **11** P10002.

2019 JINST 14 P03010